

Lithium intercalation into TiS_2 cathode material: phase equilibria in a Li– TiS_2 system

Evgeny A. Suslov¹ · Olga V. Bushkova¹ · Elena A. Sherstobitova^{1,2} · Olga G. Reznitskikh¹ · Alexander N. Titov^{2,3}

Received: 2 September 2015 / Accepted: 20 September 2015 / Published online: 17 October 2015
© Springer-Verlag Berlin Heidelberg 2015

Abstract Lithium-intercalated titanium disulfide Li_xTiS_2 had been extensively studied as prototypical cathode material for high-energy-density reversible lithium batteries with moderate voltage. Today, this phase is one of the leading candidates for all-solid-state lithium batteries with durable high energy and high rate performance. However, fundamental knowledge of Li^+ insertion into TiS_2 is still incomplete; available information on the phase diagram of the Li– TiS_2 system is limited by $x=1$ due to difficulties in preparing lithium-rich equilibrated samples. The goals of this work were to re-examine Li_xTiS_2 single phase boundaries and to clarify the existence of lithium-rich intercalates with $x>1$. A new preparation technique was developed to obtain 1T- Li_xTiS_2 samples as good-quality equilibrated products with desirable lithium content. Phase equilibria in a quasibinary Li– TiS_2 system were studied by X-ray diffraction, emf measurements (25 °C) and thermal analysis (25–350 °C) over a wide range of Li:Ti ratios (0 to 4).

Keywords Intercalation compounds · Material preparations · Electrochemical characterisations · XRD · Thermal analyses

Electronic supplementary material The online version of this article (doi:10.1007/s11581-015-1566-0) contains supplementary material, which is available to authorized users.

✉ Olga V. Bushkova
ovbushkova@rambler.ru

¹ Institute of High-Temperature Electrochemistry, Ural Branch of the Russian Academy of Sciences, Akademicheskaya st. 20, Ekaterinburg 620990, Russia

² M.N. Mikheev Institute of Metal Physics, Ural Branch of the Russian Academy of Sciences, Sofii Kovalevskoi st. 18, Ekaterinburg 620990, Russia

³ Ural Federal University, Mira st. 19, Ekaterinburg 620002, Russia

Introduction

Layered dichalcogenides with the general formula MX_2 (M=transition metal, X=S, Se, Te) form a group of materials that can be intercalated with a wide range of both organic and inorganic materials without undergoing major structural modifications [1–3]. The intercalation reaction is driven by charge transfer from the intercalant to the host layered compound conduction band; thus, electron-donating species can take part in such a reaction. Lithium-intercalated dichalcogenides Li_xMX_2 have been extensively studied as cathode materials for high-energy-density reversible lithium batteries, and TiS_2 is the prototypical cathode material, demonstrating all of the desired characteristics except for overall cell voltage, 1.7–2.5 V [1, 4–7]. Exxon combined TiS_2 with a LiAl anode and an organic-based electrolyte to create safe, rechargeable cells in 1977–1979 [4, 5]. Today, transition-metal-based cathode materials such as LiCoO_2 , $\text{LiNi}_x\text{Co}_y\text{Mn}_z\text{O}_2$, $\text{LiNi}_{0.53}\text{Co}_{0.3}\text{Al}_{0.17}\text{O}_2$, LiMn_2O_4 and LiFePO_4 are the most commonly used in commercial lithium-ion cells [4, 8–10]. Nevertheless, TiS_2 -based systems having favourable intercalation kinetics and high energy density (which have still not been exceeded by systems such as LiCoO_2 and LiMn_2O_4 [5]) are currently considered attractive candidates for high-power lithium batteries. Recently, it was demonstrated that titanium disulfide is a particularly interesting cathode material in conjunction with a metallic lithium anode in all-solid-state cells [11–14] or with lithiated silicon anode in Li-ion cells comprising modified liquid electrolyte [15]. Moreover, TiS_2 was incorporated as a second active component in sulfur–carbon cathodes of Li–S cells; serving as active reaction sites during cycling, TiS_2 suppresses agglomeration of sulfur and facilitates better ionic/electronic transport within the cathode structure [16, 17]. In addition to their practical importance, the Li– TiS_2 system has attracted considerable attention from theorists

because the TiS_2 host provides an important model for elucidating lithium diffusion mechanisms and the structural, elastic and electronic effects of lithium intercalation [18–25].

The goal of the present work was to investigate phase equilibria in the Li-TiS_2 system up to a Li:Ti ratio of 4 in order to re-examine Li_xTiS_2 single phase boundaries and to clarify the existence of lithium-rich phases with $x > 1$. Lithium-intercalated compounds Li_xTiS_2 were obtained by a new preparation technique based on direct reaction between Li metal and TiS_2 that does not set limits on the composition range. Because the structure of the titanium disulfide host remains essentially unchanged during lithium intercalation, X-ray data were combined with thermodynamic emf studies of phase equilibria. To evaluate thermal behaviour of the Li_xTiS_2 intercalates, DSC measurements were carried out over the range of 25–350 °C.

Lithium-intercalated titanium disulfide

Structure of titanium dichalcogenides TiX_2

Titanium disulfide, diselenide and ditelluride are isomorphous members of a group of compounds that crystallise in a characteristic 1T-CdI_2 layer structure ($P\bar{3} m1$ space group) [1]. Their structures (Fig. 1(a)) consist of stacked composite layers, each layer comprising two sheets of hexagonally close-packed chalcogenium atoms sandwiching a sheet of metal atoms. Because the primary valency is saturated within the sandwich X-Ti-X structure, adjacent layers are held together only by relatively weak van der Waals forces. The sandwich layers therefore form extended sheets running through the lattice, forming a strongly anisotropic structure. Thus, the crystals are characterised by a platy habit, with extended growth and pronounced cleavage perpendicular to the trigonal c -axis [1, 23, 26–28]. When intercalation occurs, the intercalant Li enters the van der Waals gaps between the X-Ti-X layers. The system can then be considered to be more three-dimensional [29]. Because the transfer of charge (electrons) from the intercalant Li atoms to the host TiX_2

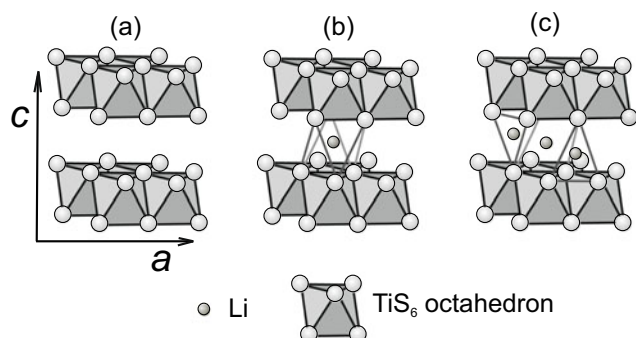


Fig. 1 Structure of $h\text{-TiX}_2$ ($\text{X}=\text{S}, \text{Se}, \text{Te}$) (a) and sequential lithium filling of octahedral (b) and tetrahedral (c) sites in van der Waals gap

lattice occurs, the relatively weak van der Waals forces are replaced by stronger Coulomb interactions, and the lattice does not expand very much along the c direction normal to the layers.

In Fig. 1(b, c), the three interstitial sites available for Li intercalation in the van der Waals gap are shown: one octahedral, which is surrounded by six chalcogen atoms, and two tetrahedrals, which lie in the projections below and above the chalcogen atoms [1, 28]. Thus, from structural considerations, the overall limiting value of intercalated lithium in the TiX_2 structure can reach $x=3$.

Lithium intercalation into TiS_2

It is generally accepted that the reaction between lithium and titanium disulfide is the perfect intercalation reaction, with the reactant and product having the same structure over the entire range of the reaction, $0 \leq x \leq 1$, in Li_xTiS_2 [1, 4, 5, 27, 30–36]. This single phase is characterised by only a 10 % expansion of the crystalline lattice along the c -axis (perpendicular to the basal plane) and approximately 1 % along the a -axis [27, 30, 34] which is typical for solid solutions. More recently, a single phase was not excluded for a wider range, at least, up to $x=1.24$ [37]. In addition to the likely extension of this solid-solution region, the results regarding the charge–discharge profiles of Li/TiS_2 cells [38–40] make it possible to propose formation of a lithium-rich compound with $x > 1$. The range of $1 \leq x \leq 2$, with a low-voltage plateau (near 0.5 V vs. Li/Li^+) in the discharge profile, had been suggested to be a region where LiTiS_2 (accepted now as the end member of Li_xTiS_2 solid solution) and hypothetical stoichiometric Li_2TiS_2 coexist [38–41]. The intercalation process for the range $0 \leq x \leq 2$ is reversible [38, 39, 41] while electrochemical intercalation up to $x=3$ results in hysteresis [39]. It should be noted, however, that all attempts to prepare the lithium-rich Li_2TiS_2 phase to study its physical properties have been unsuccessful [38, 40]; the proposed XRD pattern of Li_2TiS_2 was obtained ex situ for electrochemically intercalated samples [38]. In contrast, Li_xTiS_2 solid solutions with $0 \leq x \leq 1$ have been repeatedly synthesised and studied [1, 27, 34, 42, 43].

Thus, it is valid to say that despite numerous studies on lithium intercalation into TiS_2 , the phase diagram of the Li-TiS_2 quasibinary system clearly requires further investigation. This is particularly true for Li:Ti ratios greater than 1, for which very poor previous information (mainly, charge–discharge profiles) is available. It seems that a key problem on this way is synthesis of lithium-rich intercalate samples.

Li_xTiS_2 preparation methods

Commonly used electrointercalation in Li/TiS_2 cells with a non-aqueous electrolyte [1, 22, 30, 44–46] inevitably yields a composite product, Li_xTiS_2 , with a polymer binder,

acetylene black, electrolyte, etc. Therefore, a number of chemical intercalation techniques using non-aqueous solutions of lithiating reagents have been proposed to prepare pure Li_xTiS_2 intercalate compounds with a preset Li:Ti ratio. One such technique is the treatment of parent TiS_2 with a solution of lithium in liquid ammonia at low temperatures followed by heat treatment at 250 °C in vacuo to remove NH_3 molecules inserted between the S–Ti–S layers [1, 42, 47, 48]. In addition to ammonia co-intercalation, this technique is characterised by obvious experimental difficulties. Therefore, the most frequently used chemical intercalation technique to date remains the immersion of TiS_2 powder in the appropriate amount of *n*-butyllithium solution in hexane (or other simple hydrocarbons) for a few days [1, 18, 31, 37, 47–54]. The procedure is carried out at ambient temperatures. After the filtration and washing of the solid with hexane, vacuum drying is used to remove residual solvent. It is a “clean” method: only lithium penetrates between the layers, the butyl radicals combining to yield *n*-octane, which is easily eliminated together with the solvent. It is worth noting, however, that this method allows the maximum possible reaction product of one lithium per titanium [34], i.e. only Li_xTiX_2 with $0 < x \leq 1$, to be obtained in such a way. Only two pure intercalate samples with *x* greater than one, $\text{Li}_{1.24}\text{TiS}_2$ and $\text{Li}_{1.49}\text{TiS}_2$, have been reported in the literature [37]. A more vigorous preparation technique was used in this case; specifically, a lithium naphthalide solution in tetrahydrofuran was used as the Li source, and longer equilibration times were used during preparation (2 weeks).

The most common chemical intercalation technique using *n*-butyllithium solutions allows for good-quality Li_xTiS_2 products suitable for the measurement of physical properties to be obtained. However, such procedure without subsequent long-term heat treatment can yield inhomogeneous products due to the non-uniform distribution of intercalated Li. The direct intercalation path from the crystal surface through the X–Ti–X sandwich into the van der Waals gap is hindered by a high-energy barrier (3.81 eV for TiSe_2 [55, 56]). Therefore, the intercalation reaction occurs predominantly at the edge of the crystalline platelets, and the filling of the edges is faster than the propagation of the diffusion front into the solid [28, 53, 54, 56–58]. This leads to a bottleneck at the edges [58]. The blocking effect of intercalated lithium leads to the characteristic appearance of the Li concentration profile. This phenomenon was demonstrated by direct measurements of Li concentration profiles on titanium disulfide single crystals [54]. At room temperature, the homogenisation process is inhibited during the initial phase because the lattice has to be stretched along the stacking direction (*c*-axis) by the first lithium ions that enter. Therefore, it is necessary to homogenise the lithium distribution by heating the samples for a few days at elevated temperatures before studying the Li_xTiS_2 intercalate properties [58]. It is crucial to note that the majority of structure and physical properties investigations described in

literature were performed on the Li_xTiS_2 samples not subjected to heating.

Another way to prepare Li_xTiS_2 intercalate compounds is solid-state reactions at elevated temperatures which provide equilibrated lithium distribution. As it was shown [38, 59], Li_xTiS_2 intercalates can be synthesised from Li_2S , Ti and S as starting materials. Reagents were mixed together and placed in a carbon-coated quartz tube that was then sealed under vacuum and heated at 750 °C for 3 days, cooled slowly to 250 °C and subsequently quenched in air. This procedure was repeated again after grinding and pressing the samples. Unfortunately, lithium-deficient product relative to the desirable intercalate composition was obtained: Li_zTiS_2 ($z \approx 0.8$) instead of the set composition of LiTiS_2 [38]. When a stoichiometric mixture of the same starting materials in a sealed evacuated silica glass tube was heated at 800 °C for 2 weeks and then rapidly quenched to ambient temperature, the 3R- LiTiS_2 polymorph of LiTiS_2 was obtained instead of the 1T phase [60]. Compared to the 1T type, the 3R type shows a different stacking sequence of the sulfide layers, and the unit cell of the 3R phase is nearly three times that for the 1T phase [60, 61]. Solid-state reaction of TiS_2 with Li_2S and Ti powders at 500 to 900 °C in a sealed glass tube [61] or graphite ampoule under an argon atmosphere [62] leads to the same result: 3R- Li_xTiS_2 , 1T- Li_xTiS_2 or their mixture was obtained depending on synthesis conditions and cooling rate. Samples prepared from Li_2CO_3 and TiS_2 under the same conditions (500–900 °C, argon atmosphere) showed similar phase compositions (3R- Li_xTiS_2 , 1T- Li_xTiS_2 or their mixture) and the presence of some oxygen-containing impurity compounds [62]. It is evident from the above that solid-state synthesis at 500–900 °C makes it possible to obtain the metastable 3R- Li_xTiS_2 polymorph instead of the desired 1T- Li_xTiS_2 phase and does not guarantee a preset composition of the intercalate. Recently, ambient temperature and pressure solid-state mechanochemical lithiation technique was proposed to obtain nano- LiTiS_2 [11]; a stoichiometric mixture of TiS_2 and Li_3N was used as starting material. The resulting product had poor crystallinity.

All the studies cited above (except for [37]) suffer from the fact that lithium content in the synthesised Li_xTiS_2 intercalate samples does not exceed $x=1$. Thus, an alternative preparation technique is clearly required to re-investigate the phase diagram of the Li– TiS_2 system. Such a technique must allow obtaining equilibrated samples with the desirable lithium content over a wide range of Li:Ti ratios without any limitations and exclude formation of metastable 3R- Li_xTiS_2 intercalates.

Experimental

The TiS_2 powder (both Aldrich (99.9 %) and home-made) and lithium metal (99.9 %, Novosibirsk Chemical Concentrates Plant) were used as starting materials for the synthesis of the

lithium intercalate samples with Li:Ti ratio 0.05 to 4. Before use, lithium metal was subjected to additional purification from its degradation products by refusion. Home-made polycrystalline TiS_2 was prepared from the elements titanium (after iodine purification, 99.96 %) and sulfur (OSCh 16-5, 99.999 %) (Petersburg Krasnij Khymik Plant). The appropriated amounts of titanium and sulfur with a small excess (~3 wt%) of the latter were sintered at a temperature of 800 °C for 10–12 days in a sealed quartz ampoule evacuated down to 10^{-5} Torr. Then, the ampoule was cooled, transferred into a glove box with inert argon atmosphere and opened. The charge was ground into powder, pressed, placed into a quartz ampoule together with the same excess of sulfur (for homogenising and saturation by chalcogen), evacuated down to 10^{-5} Torr and annealed again for 10–12 days at 600 °C. After cooling, the ampoule was opened within the glove box and the charge was ground into powder. The homogeneity and a phase uniformity of the resulting product TiS_2 were tested by X-ray analysis (ICDD-ICPDS card no. 15-853). The concentration of excess titanium in the TiS_2 product thus obtained was estimated as 1 %. Online Resource 1 illustrates TiS_2 structure and morphology for home-made and Aldrich products (Figs. A1 and A2, respectively).

X-ray patterns of starting titanium disulfide and their lithium-intercalated products were obtained using Rigaku D-MAX-2200V diffractometer with a vertical goniometer (Cu $K\alpha_1$ radiation, $2\theta=5\text{--}90^\circ$). The powdered samples were placed into a sample holder of the diffractometer which was sealed with 15 μm Al foil or 30 μm Kapton tape to insulate air-sensitive samples; the foil or tape was tightly glued using two-sided scotch tape along the perimeter of the cell. The cells for XRD measurements were assembled under an argon atmosphere within a UNILAB MBRAUN glove box. The lattice parameters of TiS_2 and lithium-intercalated products Li_xTiS_2 were determined using FPEAK and/or ASTM software.

To control the lithium content in the lithium-intercalated products Li_xTiS_2 , quadrupole mass spectrometer ELAN 9000 (PerkinElmer SCIEX) was used. The ionisation is carried out by means of micro-wave plasma. The plasma jet is fed with fine aerosol of sample solution. Fine aerosol was obtained by pneumatic dispersion of the solution and subsequent separation of the raw aerosol in a temperature-stabilised Scott chamber. Sample solutions for ICP/MS analysis were obtained by dissolution of ~15 mg of Li_xTiS_2 powder in 50 ml of $\text{HCl}/\text{HNO}_3/\text{HF}=0.5:1:1$ (vol.) mixture of 0.1 M acids followed by dilution with bidistilled water by 20 times. The relative error of the x value determination by ICP/MS analysis was about 1–2 %.

The morphology of the starting TiS_2 powders and Li_xTiS_2 samples was observed using a 3 LMU (Tescan) scanning electron microscope.

Thermal behaviour of the Li_xTiS_2 intercalates was studied by differential scanning calorimetry (DSC 204 F1 Phoenix,

NETZSCH). For DSC measurements, the powder Li_xTiS_2 samples were placed and compacted into high-pressure stainless steel crucibles; then, the crucible was thoroughly screwed by the lid with gold seals. The manipulations were carried out in a dry argon atmosphere UNILAB MBRAUN box. The DSC measurements were performed in the temperature range from 25 to 350 at a heating rate of 10 °C/min and subsequent cooling in the same temperature range; the sample cell was purged with argon at a rate of 30 ml/min. The measurements for each sample were repeated at least three times. The data obtained were processed using the NETZSCH Proteus software.

The open-circuit voltage for lithium-intercalated samples with nominal composition of Li_xTiS_2 was measured at 25 °C in hermetically sealed two-probe test cells $\text{Li}|\text{SPE}|\text{Li}_x\text{TiS}_2$. Solid polymer electrolyte (SPE) used was elastomeric random copolymer of butadiene and acrylonitrile (PBAN), 60 and 40 wt% of each monomer, respectively, containing LiClO_4 [63]. The SPE conductivity at room temperature was about $10^{-3}\text{ Sm cm}^{-1}$. The Li_xTiS_2 electrodes were prepared by pressing powdered samples into a Ni grid (current collector). The area of the cathode/electrolyte interface used in the cells was about 0.5 cm^2 . The anode was the freshly scraped 1-cm-diameter lithium disc with 1 mm thickness pressed into the Ni grid. For contact improvement in the electrode/electrolyte interfaces, the assembled cells were subjected to short-term heating up to 45 °C (30 min) and then were stored at 25 °C for several days for equilibration before emf measurements. All sample preparation procedures and assembling of test cells were carried out within the dry box. A V7-34A voltmeter and P-8S Elins potentiostat with large internal resistance were used for emf measurements.

Results and discussion

The ampoule synthesis of intercalate compounds

A novel preparation technique was developed in the present work to obtain lithium-intercalated disulfide samples at a Li:Ti ratio of up to 4. To get the best results, two different preparation schemes were applied.

TiS_2 powder and Li metal were used as starting materials to synthesise samples with integer values of x (1, 2 and 3) as well as samples with Li:Ti ratios exceeding 3 (see Table 1). The precise stoichiometric amounts of the starting materials were placed in a BeO crucible (inert in respect of lithium) such that lithium metal granules measuring approximately 0.3–0.5 cm in diameter were uniformly distributed in a disulfide powder; the reaction mixture was then manually compacted to improve the contact between reagents. The BeO crucible with the reaction mixture was then placed in a Pyrex ampoule, which was evacuated to 10^{-5} Torr and sealed. The regime of the following

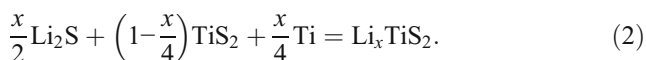
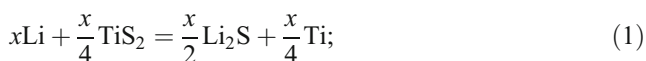
Table 1 Synthesis conditions and resulting lithium content for Li_xTiS_2 intercalate samples with integer-valued Li:Ti ratios and $\text{Li:Ti}>3$ (scheme 1)

Preset Li:Ti ratio	Starting materials	Stage 1		Stage 2		Li/Ti ratio by ICP/MS data ^a
		Temperature, °C	Time, days	Temperature, °C	Time, days	
1.0	TiS_2+Li	235	14	235	14	0.97–1.01
2.0					14	2.13
3.0					28	2.99–3.08
3.1; 3.2; 3.4					28	
4.0					35	

^a The interval of values is given for a series of syntheses

thermal treatment for each reaction mixture is presented in Table 1 for stage 1. After the first stage of annealing (when Li metal was fully transformed), the ampoules were cooled, transferred into a glove box with an inert argon atmosphere and opened. The charges were ground into powder for homogenisation, pressed into pellets and placed into Pyrex ampoules, evacuated to 10^{-5} Torr, and annealed again at the same temperatures (Table 1, stage 2). The stage 2 operations were repeated until the diffractogram of the product stopped changing; the overall durations of the thermal treatment are presented in Table 1.

Since we have proposed here a novel preparation technique for the Li_xTiS_2 intercalates, it is of interest to consider a sequence of chemical reactions, occurring in the reaction mixture during thermal treatment. An example of changes in XRD patterns during thermal treatment is shown in Fig. 2(a, b) for reaction mixture of Li metal and TiS_2 with a Li:Ti ratio of 3. The resulting chemical processes may be schematically summarised as follows:



Equation (1) describes the reaction which is the main content of stage 1 of the synthesis process while Eq. (2) relates to the interaction which proceeds mainly during stage 2. Intermediates in such a way are Li_2S and $h\text{-Ti}$ metal (incorporation of excess titanium into the van der Waals gap of TiS_2 also cannot be excluded). It is easy to see that stage 2 is chemically identical to the process used in some solid-state preparation techniques [38, 59–62] described above in Section “ Li_xTiS_2 preparation methods” but occurs at a much lower temperature due to fine $h\text{-Ti}$ intermediate (for this reason, $h\text{-Ti}$ peaks are hardly distinguishable in XRD patterns; see Fig. 2(a)) or excess Ti in $\text{Ti}_{1+y}\text{S}_2$.

Because the sample preparation technique employed can influence the experimental results (as it was shown in Section “ Li_xTiS_2 preparation methods”), it is necessary to specify some of the details of the thermal treatments. A muffle furnace with a uniform distribution of temperature along vertically placed ampoules was used to prevent a violation of

stoichiometry due to the deposition of chalcogen vapour on the cooler end of the ampoules. After each thermal treatment was completed, the ampoules were slowly cooled together with the muffle furnace to room temperature to prevent the quenching of the high-temperature phases. In all cases, any

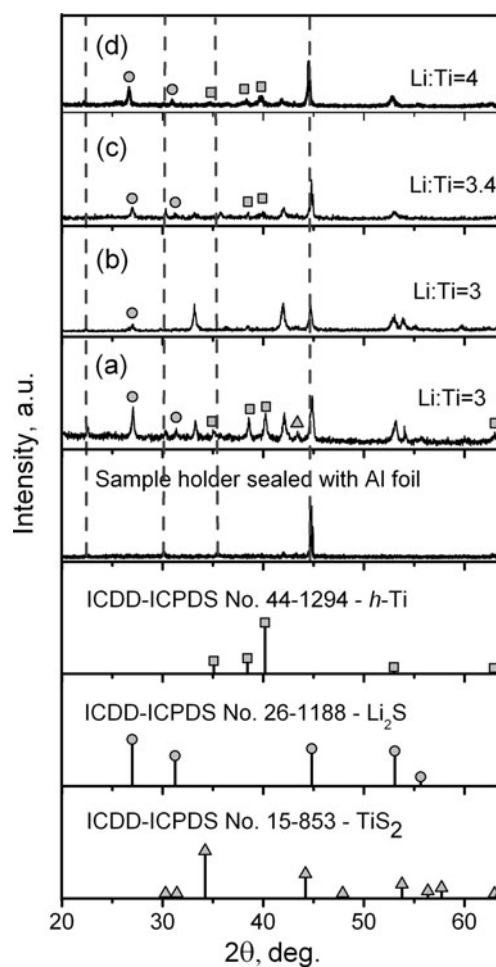


Fig. 2 XRD patterns for the reaction mixture of Li metal and TiS_2 with different Li:Ti ratios after annealing at 235 °C: *a* thermal treatment for 28 days (intermediates for Li:Ti=3); *b* thermal treatment for 42 days ($\text{Li}_3\text{-}_8\text{TiS}_2$ as a final product); *c* thermal treatment for 42 days (equilibrium products for Li:Ti=3.4); *d* thermal treatment for 49 days (nearly equilibrium products for Li:Ti=4). The dashed grey bar at the abscissa indicates the reflections from the sample holder sealed with Al foil

deposits on the ampoule walls or their turbidity due to chemical interactions with lithium vapour were absent. Therefore, it was reasonable to propose that the resulting product composition was similar to the preset value. To be confident in the composition for the intercalates obtained, the lithium content for samples with nominal compositions of LiTiS_2 , Li_2TiS_2 and Li_3TiS_2 was analysed by ICP/MS, as described in Section “**Experimental**”. The results are presented in Table 1. One can see that the uncertainty in composition associated with ampoule synthesis was approximately 1–7 %.

Li_xTiS_2 intercalates with fractional x values less than 3 were synthesised as follows. Powdered TiS_2 and synthesised products with nominal compositions of LiTiS_2 , Li_2TiS_2 and Li_3TiS_2 were used as starting materials (Table 2) to minimise the error in the preset x values, which is extremely important if taking into account a small increment in the lithium composition $\Delta x=0.05$ – 0.20 . Stoichiometric amounts of the reagents were homogenised, pressed into pellets, placed into Pyrex ampoules, evacuated to 10^{-5} Torr and then annealed at 235°C (Table 2). These operations were repeated until the diffractograms of the products stopped changing.

After completing the synthesis, all lithium-intercalated products were stored in an argon glove box for 0.5–1 year at room temperature for equilibration.

Phase composition of lithium-intercalated products

XRD patterns of the samples with Li:Ti ratio 0 to 3 are shown in Fig. 3. The formation of 1T phase with a nominal composition of Li_xTiS_2 without any impurities of the starting materials or foreign phases (including $3\text{R-Li}_x\text{TiS}_2$) was observed for all samples with $x < 3$. The sample with nominal composition of Li_3TiS_2 contained trace amounts of Li_2S , and the result was reproduced on repeated syntheses irrespective of the starting TiS_2 , Aldrich or home-made. For samples with higher lithium contents (Li:Ti > 3), titanium metal and Li_2S were found together with Li_xTiS_2 phase, and the intensity of the Ti and Li_2S peaks increased with the Li:Ti ratio (Fig. 2(c, d)). It is reasonable to conclude that the limiting intercalated lithium content in the TiS_2 structure can be really close to the expected value of $x=3$ (see Section “**Structure of titanium dichalcogenides TiX_2** ”). Intercalated lithium content in this sample may be expressed as $x=3-\delta$, with $\delta < 0.2$ taking into account Δx value (see Table 2). For the sample with Li:Ti=4 (for which XRD patterns did not stop to change for the time of the thermal treatment and, therefore, which failed to reach the equilibrium state), the lithium-intercalated phase tended to disappear (Fig. 2(d)). Because of this, Ti and Li_2S must be equilibrium products; this conclusion is consistent with thermodynamic estimations of stable two-phase lines in isothermal ternary cross section of the Li–Ti–S system [37].

XRD data (Fig. 3) indicate the minor changes of the Li_xTiS_2 diffraction profiles with lithium content over the entire

range of the lithium intercalation, $0 \leq x \leq 3$. Figure 4 gives the details of the variation of (001) Bragg peak (one of the most sensitive to c -axis expansion) as a function of Li content. One can see that the magnitudes of the shifts in the peak positions that occur upon intercalation are very small and become zero at $x \geq 1$; no noticeable splitting of the (001) peak is observed over the whole concentration range $0.05 \leq x \leq 3.0$. Because the structure of the TiS_2 host remains essentially unchanged during lithium intercalation, the distinction between coexisting intercalate phases within two-phase regions (if this is the case) can hardly be detected by XRD. Therefore, XRD alone is not an appropriate tool to establish the exact phase composition of the intercalate samples with a nominal Li_xTiS_2 composition, i.e. for $x \leq 3$. Consequently, thermodynamics studies have to be performed as a more precise tool in the investigation of phase equilibria in this very specific Li– TiS_2 system. In the present work, emf data were used to construct the phase diagram.

Emf measurements

The emf technique is known to be an excellent tool of solid-state chemistry that allows for direct measurements of the thermodynamic parameters of the intercalation process [1, 25, 64–67]. For studies of lithium intercalation into titanium disulfide host, a simple reversible two-electrode test cell $\text{Li} | \text{electrolyte} | \text{Li}_x\text{TiS}_2$ can be used, in which the negative electrode (lithium metal), which exhibits a constant voltage, also serves as a reference electrode. The equilibrium voltage difference between the two electrodes separated by a Li^+ -conducting electrolyte in an open-circuit is the electromotive force of the cell, $V(x)$. At a fixed temperature, emf is a function of lithium content x in a chemically formed intercalate with a nominal composition of Li_xTiS_2 and depends on the difference in the Li chemical potential between the anode and cathode according to the Nernst equation [6, 25, 65]:

$$V(x) = -\frac{\mu_{\text{Li}}^{\text{cathode}}(x) - \mu_{\text{Li}}^{\text{anode}}}{zF} = -\frac{\Delta\bar{G}(x)}{zF}. \quad (3)$$

$\mu_{\text{Li}}^{\text{cathode}}(x)$ is the Li chemical potential in Li_xTiS_2 , $\mu_{\text{Li}}^{\text{anode}}$ is the Li chemical potential in the lithium metal anode, F is the Faraday constant and $z=1$ is the charge (in electrons) transported by lithium in the electrolyte. It is clear that the cell emf under isothermal and isobaric conditions is defined by the lithium chemical potential in a Li_xTiS_2 sample only. The value of $V(x)$ at a given temperature measures the change in the molar Gibbs free energy of intercalation $\Delta\bar{G}(x)$ in the reversible reaction



Therefore, the composition dependence of emf provides direct thermodynamic information about phase equilibria in the Li– TiS_2 system. As Li is intercalated, its chemical potential in the cathode increases, leading to a decrease in the cell

Table 2 Synthesis conditions for intercalates with nominal composition of Li_xTiS_2 and fractional x values less than 3 (scheme 2)

Preset x value	Δx	Starting materials	Synthesis conditions	
			Temperature, °C	Time, days
0.05 to 0.90	0.05–0.1	$\text{TiX}_2 + \text{LiTiS}_2^a$	235	14
1.1 to 1.8	0.2	$\text{TiX}_2 + \text{Li}_2\text{TiS}_2^a$		
2.2 to 2.8	0.2	$\text{TiX}_2 + \text{Li}_3\text{TiS}_2^a$		28

^a Nominal compositions

voltage. The continuous decrease in emf with increasing x is characteristic of a single-phase system and indicates solid-solution behaviour. Coexisting phase regions (first-order phase transformation) appear as plateaus in emf vs. x plots because the chemical potential of Li in coexisting phases is equal. Second-order phase transitions that do not involve two-phase domains can even be detected, as they lead to changes in the slope of the voltage curve [1, 25, 64, 65, 67–70].

The critical issues encountered in emf investigations are as follows. It is necessary to prevent any foreign chemical processes from occurring on the electrode/electrolyte interfaces to eliminate any “parasitic” contribution to the measured open-circuit voltage (OCV) value. Thus, a solvent-free Li^+ -conducting solid polymer electrolyte [63] chemically stable in contact with lithium metal was used in our experiments. Emf measurements were carried out under isothermal conditions (25 °C) for long durations (up to

1–3 days) until the cell OCV stopped changing; the final value was accepted as the emf. To verify the reproducibility of the emf results, a series of electrochemical cells (from 2 to 6) was assembled for each Li_xTiS_2 intercalate sample. Moreover, a repeat synthesis with different TiS_2 hosts, Aldrich and home-made, was performed for some samples (Li_xTiS_2 with $x=1$ and 3) to verify the reproducibility of the results. To test the results obtained for equilibrium, cell OCV measurements were carried out at 25 °C as described above before and after thermal treatment at 50–95 °C. Finally, it should be particularly emphasised that the intercalated samples under investigation were prepared such that the equilibrium lithium distribution was guaranteed.

The emf vs. x dependencies for intercalates with nominal compositions of Li_xTiS_2 ($0 \leq x \leq 3$) as well as for three-phase samples with $\text{Li}:\text{Ti} > 3$ are shown in Fig. 5(a), where all emf values obtained are presented. One can see that the reproducibility of the emf measurements is rather good in spite of the different starting TiS_2 for Li_xTiS_2 synthesis, home-made or Aldrich. Therefore, we can conclude that the careful control described above made it possible to obtain thermodynamic emf results that truly characterise phase equilibria in the Li– TiS_2 system.

Phase equilibria in the Li– TiS_2 system

The emf vs. x dependence for the Li– TiS_2 system at 25 °C (Fig. 5(a)) can clearly be divided into five different regions that reflect changes in phase composition with lithium content. Regions I ($0 \leq x \leq 0.30$) and III ($0.80 \leq x \leq 1.4$), where a

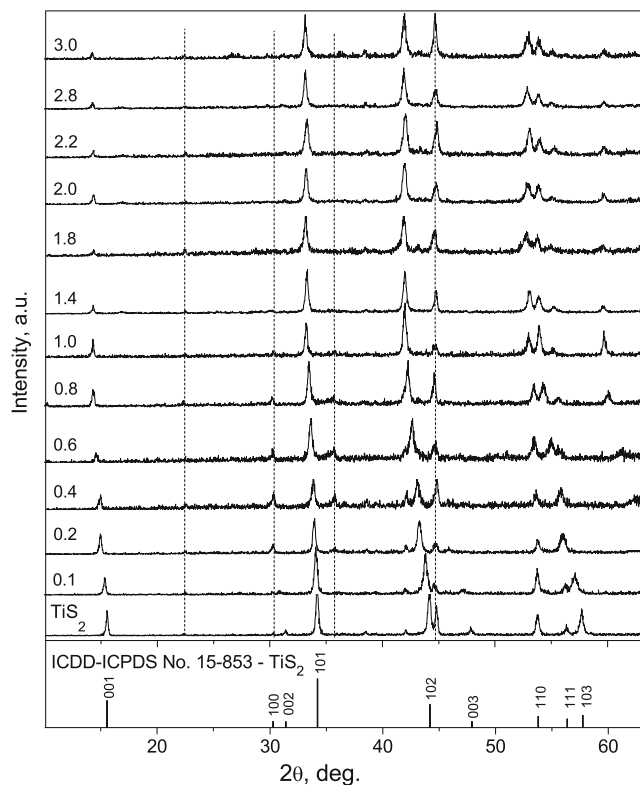


Fig. 3 XRD patterns for TiS_2 and lithium-intercalated disulfide samples with varied Li:Ti ratios (indicated on the left). The dashed grey bar at the abscissa indicates the reflections from the sample holder sealed with Al foil

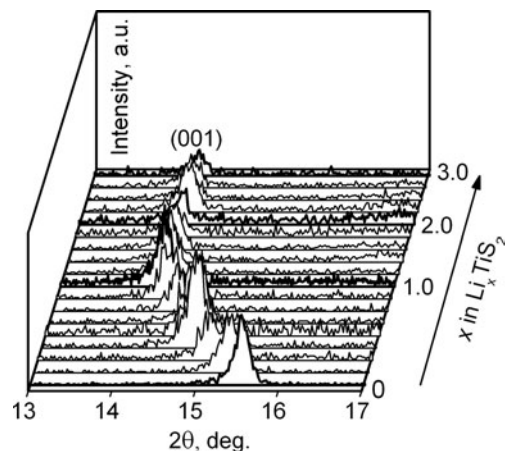


Fig. 4 Variation of (001) Bragg peak as a function of x in Li_xTiS_2

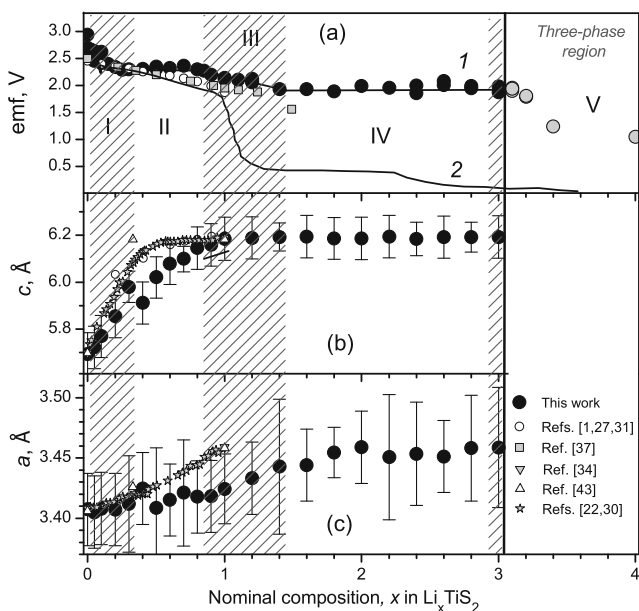


Fig. 5 Concentration dependencies of emf (a) and lattice parameters c (b) and a (c) for lithium-intercalated titanium disulfide at 25 °C. 1—emf concentration dependence obtained in this work; 2—discharge profile of Li/TiS_2 cell at room temperature [39]. Lattice parameters are shown for sample series prepared from TiS_2 (Aldrich). The solid bar at the abscissa indicates the intercalation limit of $x=3$ for Li_xTiS_2 ; the shaded areas correspond to solid-solution regions

decrease in emf is observed must be attributed to solid-solution behaviour. Region II (between $x=0.30$ and $x=0.80$), with a constant emf of approximately 2.30 V, can be associated with two-phase system behaviour corresponding to the coexistence of the end members of these two solid-solution series. The voltage plateau at ~ 1.95 V between $x=1.4$ and $x=3.0$ (region IV) is indicative of the coexistence of two phases as well and suggests the formation of a lithium-rich intercalated compound with nominal composition of Li_3TiS_2 . The existence of the Li_2TiS_2 phase proposed previously [38–41] lacks support from the emf vs. x dependence obtained in our work. When the Li:Ti ratio exceeds the proposed upper lithium intercalation limit of 3, a sharp decrease in emf is observed within three-phase region V, composed of lithium-rich Li_3TiS_2 phase, Li_2S and Ti metal.

Figure 5(b, c) shows the variation in the lattice parameters a and c as a function of x for the lithium intercalation range $0 \leq x \leq 3$ together with the emf (Fig. 5(a)). The characteristics of the a and c dependencies agree with the emf results, but it is easily observed that the lattice parameters alone do not provide reliable information on phase equilibria in the Li– TiS_2 system due to the small amplitude of the structure changes (see also Fig. 4).

Li_xTiS_2 single phase within the $0 \leq x \leq 0.30$ range is clearly based on the parent TiS_2 structure. Lithium intercalation is accompanied by a linear increase in the c lattice parameter but does not cause any changes in a (Fig. 5(b, c)). Such behaviour is known to be caused by preferential Li insertion into

the octahedral sites of the van der Waals gap, which follows from NMR and neutron diffraction results as well as theoretical calculations [18, 25, 31, 34, 71]. The characteristic feature of single-phase Li_xTiS_2 within the range $0 \leq x \leq 0.30$ is the abrupt change in the slope of the emf vs. x curve in the vicinity of $x=0.10$ (Fig. 5(a)), which may be indicative of a second-order phase transition.

The next solid-solution range extending from $x=0.80$ to 1.4 can be regarded as a continuous, homogeneous region of LiTiS_2 phase. For $x=1$, all octahedral sites must be occupied, but a small percentage of Li ions might reside in tetrahedral sites also [34, 36]. The intercalation energy was established to be larger at the octahedral positions than at the tetrahedral ones, but the difference between the two positions decreases as x increases [18]; therefore, tetrahedral sites become energetically attractive as well. Because there is only one octahedral site for Li per TiS_2 unit, tetrahedral positions have to be populated for $1 < x \leq 1.4$ as well. As shown in Fig. 5(b), the c parameter stops changing and a plateau is observed when all octahedral sites become filled at $x=1$. Thus, the partial filling of tetrahedral sites does not cause any increase in the c lattice parameter, whereas the a parameter appears to be sensitive to lithium insertion into tetrahedral sites and increases with x , although very slightly ($\sim 1\%$, Fig. 5(c)). An increase in the a parameter within continuous LiTiS_2 -based solid-solution range (region III) results from Coulomb repulsion between ionised Li atoms intercalated into TiX_2 crystal lattice [47, 72]. Since Δa is very small, it is reasonable to propose that the effect of Coulomb repulsion is small. An increase in the value of a within two-phase region IV, between $x=1.4$ and $x=3$ (Fig. 5(c)), must be attributed to the poor resolution of reflections from LiTiS_2 -based solid solutions (see Fig. 3).

In a stoichiometric phase of Li_3TiS_2 , both octahedral and tetrahedral sites in the van der Waals gap of the host TiS_2 lattice would have been fully occupied by lithium. Since Li_2S traces were detected for all XRD patterns of the samples with the nominal composition of Li_3TiS_2 at repeated syntheses (see Figs. 2(b) and 6), we had proposed that the real lithium content in this phase corresponds to $3-\delta$ (as discussed in Section “Phase composition of lithium-intercalated products”). This result seems to be quite reasonable, because the more completed the octa- and tetrahedral sites are, the more difficult it becomes for lithium to intercalate into the compound structure. Therefore, Li_3TiS_2 corresponds to the limiting phase composition, which is unlikely to be achieved in a real synthesis procedure. The filling of two tetrahedral sites after octahedral ones does not cause any increase in the c lattice parameter relative to that measured for LiTiS_2 (Fig. 5(b)), whereas the a lattice parameter increases by 1.4 % and reaches its maximum at $x=3$ (Fig. 5(c)). More detailed characterisation of synthesised samples with nominal composition of Li_3TiS_2 is given in Online Resource 2. In order to establish real lithium content and Li atom distribution in the structure of this new Li-rich phase obtained for the

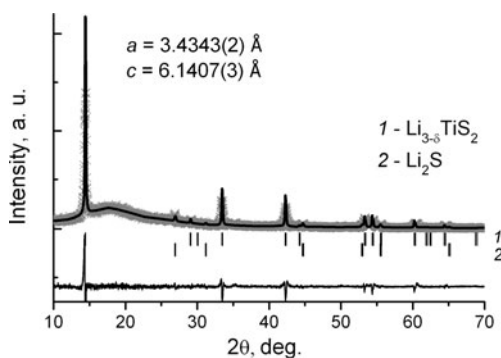


Fig. 6 XRD pattern of sample with nominal composition of Li_3TiS_2 prepared from home-made TiS_2

first time, high-resolution neutron diffraction measurements are obviously needed. This will be done soon and described in a forthcoming paper.

It is appropriate to correlate the composition dependencies of the emf and lattice parameters obtained in the present work with other data sets available from the literature and also presented in Fig. 5. In making this comparison, it should be recalled following sample preparation features. Firstly, home-made TiS_2 powders with distinct deviations from stoichiometry were used as starting materials in all cited works; secondly, different sample preparation techniques were applied to obtain Li_xTiS_2 products. Therefore, the discrepancy in the lattice parameters of Li_xTiS_2 (Fig. 5(b, c)) seems to be inevitable. The discrepancy in the emf values also is not surprising since they are very sensitive to lithium distribution. All literature data (Fig. 5(a)) were collected from samples lithiated chemically using *n*-butyllithium near room temperature without annealing [1, 27, 31, 34, 37, 43] or electrochemically [22, 30]. An inhomogeneous lithium distribution in samples thus obtained was particularly noted by Dahn et al. [34] and Hibma [72] and more recently discussed in detail by Winter and Heitjans [58] and Schwarzburger et al. [54]. Our results, in contrast, were obtained from equilibrated Li_xTiS_2 samples. It is worth noting, however, that the emf values within the first solid-solution range ($0 \leq x \leq 0.3$) are nearly identical despite the differences in the preparation technique employed. Moreover, this part of emf vs. *x* dependence is almost identical to the corresponding part of the discharge curve on lithium insertion into TiS_2 [39] (Fig. 5(a), curve 2). This observation may be attributed to the lack of first-order phase changes over $0 \leq x \leq 0.3$ composition range and therefore the fast homogenisation of the lithium distribution and equilibration of such samples irrespective of the Li_xTiS_2 preparation technique. In contrast, a more complicated non-equilibrium phase composition must be proposed for all samples prepared chemically with a higher lithium content of $0.3 < x \leq 1.49$ (Fig. 5). One can readily see from Fig. 5(a) that the published emf values for intercalates with a nominal stoichiometry of LiTiS_2 [1, 27, 37] are very similar to those of the hypothetical phase $\text{Li}_{3-\delta}\text{TiS}_2$ obtained in our work. This result seems to be quite reasonable because

$\text{Li}_{3-\delta}\text{TiS}_2$ may be precisely the phase responsible for the “blocking effect” (see Section “ Li_xTiS_2 preparation methods”) under lithium-rich conditions due to deficiency of lithium vacancies available for Li motion in its structure.

Phase boundaries in the Li– TiS_2 system is one more subject to be discussed in relation to information available in the literature for a nominal stoichiometry of $0 \leq x \leq 1$. It must be noted that the limits of the two solid-solution series established in our work agree with the profile of the composition dependence of magnetic susceptibility obtained for chemically lithiated and annealed (250 °C) Li_xTiS_2 samples for *x* ranging from 0 to 1 [42]. The correlation between several phase regions existing in Li_xTiS_2 and changes in the degree of lithium ionisation is also worth noting. It was established that the ionisation of the first Li atoms entering the TiS_2 host is essentially complete due to the donation of Li-conducting electrons to the lattice, while above $x=0.80$, electron transfer from Li to TiS_2 is not complete, with 10–20 % of the valence electron density remaining in the vicinity of the lithium atoms in LiTiS_2 [20, 24, 31, 32, 36, 42, 71]. Finally, two series of Li_xTiS_2 solid solutions definitely differ in their ability to exist as 3R-polymorph. So, TiS_2 -based solid solutions ($0 \leq x \leq 0.3$) correspond to composition range where formation of 3R- Li_xTiS_2 was not observed at high-temperature solid-state synthesis, and all diffraction peaks were well indexed to the 1T structure [61]. It is interesting that electrochemical delithiation of 3R- LiTiS_2 resulted in a non-reversible transformation to the 1T phase at $x \leq 0.4$ [62]. It is likely, therefore, that the 3R phase is a polymorph of the LiTiS_2 -based solid solutions only ($0.80 \leq x \leq 1.4$).

The correlation between phase boundaries established in the present work and the results obtained by the incremental capacity technique [30, 44, 45] also merits discussion. A principal feature of this peculiar data collection scheme proposed by Thompson [44, 45] is that both kinetic and thermodynamic data can be collected during the same measurement. Although the voltage vs. composition curves for Li/ Li_xTiS_2 cells [30, 44, 45] are not identical to our thermodynamic emf results, the peaks in the $-\Delta x/\Delta V$ vs. *x* dependencies at $x=1/9$, $1/4$ and $6/7$ are very similar to our phase boundary values. The reason for such correlation is still unclear, taking into account the inevitable effect of kinetics during incremental capacity measurements. The peaks at these fractional compositions are usually interpreted by assuming that ordered superlattices exist for the Li ions and vacancies [30, 44, 45]; lattice-gas theory was used to justify this assumption. It is possible that superlattice formation is actually the cause of the first- and second-order phase transitions in Li_xTiS_2 intercalates, but a more detailed study is beyond the scope of this work.

Li–Ti–S isothermal ternary section

New results regarding phase equilibria in the quasibinary Li– TiS_2 system at 25 °C allow for the clarification of the

isothermal ternary section Li–Ti–S proposed previously by Johnson and Worrell [37]. The resulting fragment of the Li–Ti–S isothermal section is presented in Fig. 7; the data concerning phase equilibria in constituent binary systems [73–75] were also taken into account. The Li–Ti–S diagram indicates that for Li:Ti ratios greater than 3, there is three-phase region composed of Li_2S , titanium metal and $\text{Li}_{3-\delta}\text{TiS}_2$. For Li:Ti=4:1, two-phase equilibrium between Li_2S and titanium metal was established. A further increase in the Li:Ti ratio results in three-phase equilibrium between Li_2S , titanium metal and lithium metal.

Thermal behaviour of the Li_xTiS_2 intercalates

To investigate thermal stability of lithium-intercalated compounds, single-phase samples from different regions of the phase diagram (Fig. 7) were selected: $\text{Li}_{0.15}\text{TiS}_2$, $\text{Li}_{0.25}\text{TiS}_2$, LiTiS_2 and the sample with nominal composition of Li_3TiS_2 . DSC curves for all samples are presented in Fig. 8. It can be seen that the DSC curves do not demonstrate any effects associated with phase transitions. These data were well reproduced in repeated measurements. It is evident from the results that all intercalates studied are thermally stable in the temperature range of 25–350 °C. This is true for both TiS_2 -based ($0 \leq x \leq 0.3$) and LiTiS_2 -based ($0.8 \leq x \leq 1.4$) solid solutions as well as for hypothetical lithium-rich $\text{Li}_{3-\delta}\text{TiS}_2$ compound. A small deviation of the DSC curves above 240–300 °C may be caused by disturbance of the stoichiometry of the host lattice due to intensive reversible vaporisation of sulfur [76]. Therefore, we ought to propose authenticity of the isothermal section of the phase diagram of the ternary system Li–Ti–S, which is shown in Fig. 7 for 25 up to 350 °C.

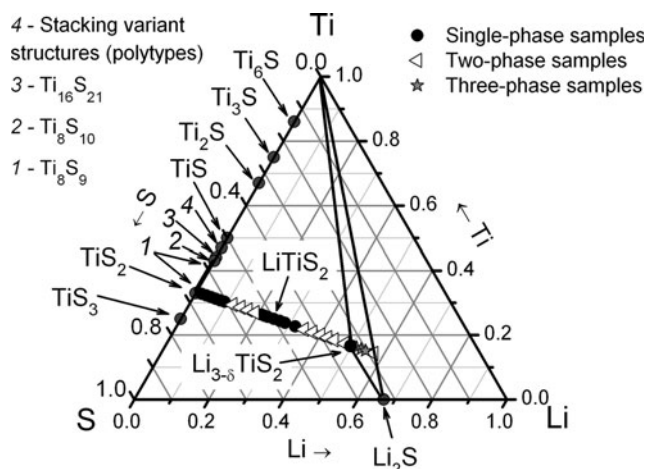


Fig. 7 Fragment of the isothermal section of the Li–Ti–S ternary system at 25 °C

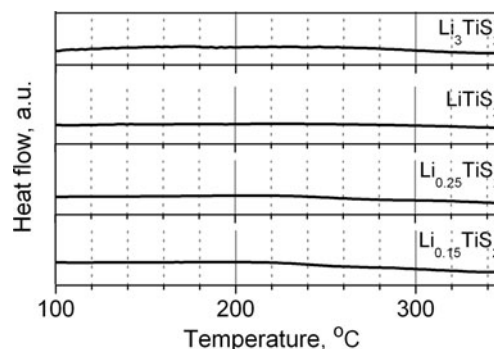


Fig. 8 DSC curves of the Li_xTiS_2 samples measured in hermetically sealed high-pressure stainless steel crucibles

Conclusion

A novel preparation technique based on direct reaction between Li metal and TiS_2 allowed obtaining a good-quality equilibrated product with a desirable lithium content over a wide range of Li:Ti ratios (0 to 4). This technique made it possible to overcome the limit of $x \sim 1.5$ previously reached for pure Li_xTiS_2 compounds and to get for the first time a lithium-rich phase with proposed composition of $\text{Li}_{3-\delta}\text{TiS}_2$. The results of re-investigations of phase equilibria in the quasibinary Li– TiS_2 system provide grounds to revise the current accepted view of the single-phase Li_xTiS_2 over the entire composition range of $0 \leq x \leq 1$ where two series of solid solutions were found.

Acknowledgments The studies were supported by the Russian Foundation for Basic Research (grant no. NK 13-03-96032\13). This work has been (partly) done using facilities of the shared access centre “Composition of compounds”, Institute of High-Temperature Electrochemistry of the Ural Branch of the Russian Academy of Sciences, and shared access centre “Elemental and isotopic analysis of solids”, Institute of Solid State Chemistry of the Ural Branch of the Russian Academy of Sciences. The authors are thankful to Dr. B.D. Antonov for the recording of XRD patterns, A.A. Pankratov for the recording of SEM images and V.T. Surikov for the elemental analysis of the samples.

References

- Whittingham MS (1978) Chemistry of intercalation compounds: metal guests in chalcogenide hosts. *Prog Solid St Chem* 12:41–99
- Julien CM (2003) Lithium intercalated compounds: charge transfer and related properties. *Mat Sci and Eng R* 40:47–102
- Whittingham MS, Ebert LB (1979) In: Levy F (ed) *Intercalated layered materials (physics and chemistry of materials with layered structures)*, vol 6. D Reidel Publishing Company, Dordrecht, pp 533–562
- Whittingham MS (2004) Lithium batteries and cathode materials. *Chem Rev* 104:4271–4301
- Thackeray MM, Thomas JO, Whittingham MS (2000) Science and applications of mixed conductors for lithium batteries. *MRS Bull* 25:39–46
- Manthiram A (2009) In: Nazri G-A, Pistoia G (eds) *Lithium batteries: science and technology*. Springer, New York, pp 3–41

7. Whittingham MS (1976) Electrical energy storage and intercalation chemistry. *Science* 192:1126–1127
8. Pasquali M, Passerini S, Pistoia G (2009) In: Nazri G-A, Pistoia G (eds) *Lithium batteries: science and technology*. Springer, New York, pp 315–380
9. Prosini PP (2011) *Iron phosphate materials as cathodes for lithium batteries*. Springer, London
10. Yoshio M, Noguchi H (2009) In: Yoshio M, Brodd RJ, Kozawa A (eds) *Lithium-ion batteries: science and technologies*. Springer, New York, pp 9–48
11. Yersak TA, Yan Y, Stoldt C, Lee S-H (2012) Ambient temperature and pressure mechanochemical preparation of nano-LiTiS₂. *ECS Electrochem Lett* 1:A21–A23
12. Trevey JE, Stoldt CR, Lee S-H (2011) High powder nanocomposite TiS₂ cathodes for all-solid-state lithium batteries. *J Electrochem Soc* 158:A1282–A1289
13. Shin BR, Nam YJ, Kim JW, Lee Y-G, Jung YS (2014) Interfacial architecture for extra Li⁺ storage in all-solid-state lithium batteries. *Sci Rep* 4:5572
14. Shin BR, Nam YJ, Oh DY, Kim DH, Kim JW, Jung YS (2014) Comparative study of TiS₂/Li-In all-solid-state lithium batteries using glass-ceramic Li₃PS₄ and Li₁₀GeP₂S₁₂ solid electrolytes. *Electrochim Acta* 146:395–402
15. Elazari R, Salitra G, Gershinshy G, Garsuch A, Panchenko A, Aurbach D (2012) Li ion cells comprising lithiated columnar silicon film anodes, TiS₂ cathodes and fluoroethylene carbonate (FEC) as a critically important component. *J Electrochem Soc* 159:A1440–A1445
16. Garsuch A, Herzog S, Montag L, Krebs A, Leitner K (2012) Performance of blended TiS₂/sulfur/carbon cathodes in lithium-sulfur cells. *ECS Electrochem Lett* 1:A24–A26
17. Su Y-S, Manthiram A (2014) Sulfur/lithium-insertion compound composite cathodes for Li-S batteries. *J Power Sources* 270:101–105
18. Bredow T, Heitjans P, Wilkening M (2004) Electric field gradient calculations for Li_xTiS₂ and comparison with ⁷Li NMR results. *Phys Rev B* 70:115111
19. Fischer JE, Kim HJ (1987) Elastic effects in intercalation compounds: comparison of lithium in graphite and TiS₂. *Phys Rev B* 35:3295–3298
20. Clerc DG, Poshusta RD, Hess AC (1997) Periodic Hartree-Fock study of Li_xTiS₂, 0 ≤ x ≤ 1: the structural, elastic and electronic effects of lithium intercalation in TiS₂. *J Phys Chem A* 101:8926–8931
21. Mendizábal F, Contreras R, Aizman A (1997) Molecular modeling of lithium intercalation in 1T-TiS₂. *J Phys-Condens Mat* 9:3011–3021
22. Dahn JR, Dahn DC, Haering RR (1982) Elastic energy and staging in intercalation compounds. *Solid State Commun* 42:179–183
23. Wang JC (1990) Model for lithium intercalation into TiS₂. *Solid State Ionics* 40(41):548–552
24. Umrigar C, Ellis DE, Wang D-S, Krakauer H, Posternak M (1982) Band structure, intercalation and interlayer interactions of transition-metal dichalcogenides: TiS₂ and LiTiS₂. *Phys Rev B* 26:4935–4950
25. Van der Ven A, Thomas JC, Xu Q, Swoboda B, Morgan D (2008) Nondilute diffusion from first principles: Li diffusion in Li_xTiS₂. *Phys Rev B* 78:104306
26. Rimmington HPB, Balchin AA (1974) The growth by iodine vapor transport techniques and the crystal structures of layer compounds in the series TiS_xSe_{2-x}, TiS_xTe_{2-x}, TiSe_xTe_{2-x}. *J Cryst Growth* 21: 171–181
27. Whittingham MS (1976) The role of ternary phases in cathode reactions. *J Electrochem Soc* 123:315–320
28. Ramírez C, Adelung R, Kunz R, Kipp L, Schattke W (2005) Lithium adsorption by TiSe₂ of varying concentration via density functional theory. *Phys Rev B* 71:035426
29. Yoffe AD (1983) Physical properties of intercalated solids. *Solid State Ionics* 9–10:59–70
30. Dahn JR, Haering RR (1981) Anomalous Bragg peak widths in Li_xTiS₂. *Solid State Commun* 40:245–248
31. Silbernagel BG, Whittingham MS (1976) An NMR study of the alkali metal intercalation phase Li_xTiS₂: relation to structure, thermodynamics and ionicity. *J Chem Phys* 64:3670–3673
32. Whittingham MS (1979) Intercalation chemistry and energy storage. *J Solid State Chem* 29:303–310
33. Leblanc-Soreau A, Danot M, Trichet L, Rouxel J (1974) Les intercalaires A_xTiS₂ et A_xZrS₂. Structure et liaisons. *Mat Res Bull* 9:191–198
34. Dahn JR, McKinnon WR, Haering RR, Buyers WJL, Powell BM (1980) Structure determination of Li_xTiS₂ by neutron diffraction. *Can J Phys* 58:207–213
35. Chianelli RR, Scanlon JC, Rao BML (1978) Dynamic X-ray diffraction. *J Electrochem Soc* 125:1563–1566
36. Kleinberg RL (1982) Electric field gradient, anisotropic shift, tetrahedral site occupation and atomic motion in Li_xTiS₂. *J Phys Chem Solids* 43:285–290
37. Johnson WB, Worrell WL (1986) Structural and thermodynamic properties of cointercalated titanium disulfide. *J Electrochem Soc* 133:1966–1970
38. Kim Y, Park K-S, Song S-H, Han J, Goodenough JB (2009) Access to M³⁺/M²⁺ redox couples in layered LiMS₂ sulfides (M=Ti, V, Cr) as anodes for Li-ion battery. *J Electrochem Soc* 156:A703–A708
39. Dahn J, Haering RR (1979) Lithium intercalation in TiS₂. *Mat Res Bull* 14:1259–1262
40. Murphy DW, Carides JN (1979) Low voltage behavior of lithium/metal dichalcogenide topochemical cells. *J Electrochem Soc* 126: 349–351
41. Dahn JR, Py MA, Haering RR (1982) In situ X-ray diffraction experiments on lithium intercalation compounds. *Can J Phys* 60: 307–313
42. Bernard L, Glaunsinger W, Colombet P (1985) Magnetic investigation of the intercalation compounds Li_xTiS₂. *Solid State Ionics* 17:81–89
43. Patel SN, Balchin AA (1983) Observation of intermediate phases during the lithium intercalation of TiX₂ (X=S, Se). *Z Kristallogr* 164:273–278
44. Thompson AH (1979) Electrochemical potential spectroscopy: a new electrochemical measurement. *J Electrochem Soc* 126:608–616
45. Thompson AH (1978) Lithium ordering in Li_xTiS₂. *Phys Rev Lett* 40:1511–1514
46. Julien C, Samaras I, Gorochoy O, Ghorayeb AM (1992) Optical and electrical-transport studies on lithium-intercalated TiS₂. *Phys Rev B* 45:13390–13395
47. Friend RH, Yoffe AD (1987) Electronic properties of intercalation complexes of the intercalation complexes of the transition metal dichalcogenides. *Adv Phys* 36:1–94
48. Rouxel J (1979) In: Levy F (ed) *Intercalated layered materials (physics and chemistry of materials with layered structures)*, vol 6. D Reidel Publishing Company, Dordrecht, pp 533–562
49. Murphy DW, Di Salvo FJ, Hull GW, Waszczak JV (1976) Convenient preparation and physical properties of lithium intercalation compounds of group 4B and 5B layered transition metal dichalcogenides. *Inorg Chem* 15:17–21
50. Whittingham MS, Gamble FR Jr (1975) The lithium intercalates of the transition metal dichalcogenides. *Mat Res Bull* 10:363–372
51. Wilkening M, Heitjans P (2008) Li jump process in *h*-Li_{0.7}TiS₂ studied by two-time ⁷Li spin-alignment echo NMR and comparison with results on two-dimensional diffusion from nuclear magnetic relaxation. *Phys Rev B* 77:024311
52. Wilkening M, K uchler W, Heitjans P (2006) From ultraslow to fast lithium diffusion in the 2D ion conductor Li_{0.7}TiS₂ probed directly

- by stimulated-echo NMR and nuclear magnetic relaxation. *Phys Rev Lett* 97:065901
53. Chianelli RR, Scanlon JC, Rao BML (1979) In situ studies of electrode reactions: the mechanism of lithium intercalation in TiS_2 . *J Solid State Chem* 29:323–337
 54. Schwarzburger NI, Knobel R, Behrens H, Binnewies M, Horn I, Pelster A, Arlinghaus HF, Dörrer L, Schmidt H (2012) Kinetics of lithium intercalation in titanium disulfide single crystals. *Z Phys Chem* 226:461–489
 55. Ramírez C, Schattke W (2001) Diffusion and intercalation of alkali atoms in transition metal dichalcogenides. *Surf Sci* 482–485:424–429
 56. Schattke W, Ramírez C (2004) Ab initio study of alkali atoms intercalation in transition metal dichalcogenide. In: Wolf D, Münster G, Kremer M (eds) *Proceedings of NIC Symposium 2004*, NIC series vol. 20. John von Neumann Institute for Computing, Jülich, pp 191–200
 57. Whittingham MS, Panella JA (1981) Formation of stoichiometric titanium disulfide. *Mat Res Bull* 16:37–45
 58. Winter R, Heitjans P (2001) Li^+ diffusion and its structural basis in the nanocrystalline and amorphous forms of two-dimensionally ion-conducting Li_xTiS_2 . *J Phys Chem B* 105:6108–6115
 59. Yang G, Kim Y, Goodenough JB (2011) The influence on Fermi energy of Li-site change in $\text{Li}_z\text{Ti}_{1-y}\text{Ni}_y\text{S}_2$ on crossing $z=1$. *J Mater Chem* 21:10160–10164
 60. Nakhal S, Lerch M, Koopman J, Islam MM, Bredow T (2013) Crystal structure of 3R-LiTiS_2 and its stability compared to other polymorphs. *Z Anorg Allg Chem* 639:2822–2825
 61. Zhang Z, Dong C, Guan C, Yang L, Luo X, Li A (2015) Sealed-tube synthesis and phase diagram of Li_xTiS_2 ($0 \leq x \leq 1$). *Mat Res Bull* 61:499–503
 62. Colbow KM, Dahn JR, Haering RR (1989) The 3R phase of Li_xTiS_2 . *J Power Sources* 26:301–307
 63. Bushkova OV, Animitsa IY, Lirova BI, Zhukovsky VM (1997) Lithium conducting solid polymer electrolytes based on polyacrylonitrile copolymers: ion solvation and transport properties. *Ionics* 3:396–404
 64. Delmas C, Ménétrier M, Croguennec L, Levasseur S, Pérès JP, Poullier C, Prado G, Fournès L, Weill F (1999) Lithium batteries: a new tool in solid state chemistry. *Int J Inorg Mater* 1:11–19
 65. Aydinol MK, Kohan AF, Ceder G, Cho K, Joannopoulos J (1997) Ab initio study of lithium intercalation in metal oxides and metal dichalcogenides. *Phys Rev B* 56:1354–1365
 66. Molenda J (2005) Electronic limitations of lithium diffusibility. From layered and spinel toward novel olivine type cathode materials. *Solid State Ionics* 176:1687–1694
 67. Zaghib K, Guerfi A, Hovington P, Vijn A, Trudeau M, Mauger A, Goodenough JB, Julien CM (2013) Review and analysis of nanostructured olivine-based lithium rechargeable batteries: status and trends. *J Power Sources* 232:357–369
 68. Dahn JR (1991) Phase diagram of Li_xC_6 . *Phys Rev B* 44:9170–9177
 69. Reynier Y, Yazami R, Fultz B (2003) The entropy and enthalpy of lithium intercalation into graphite. *J Power Sources* 119–121:850–855
 70. Lee H-H, Wan C-C, Wang Y-Y (2003) Identity and thermodynamics of lithium intercalated in graphite. *J Power Sources* 114:285–291
 71. Kleinberg RL, Silbernagel BG (1980) Lithium motion in $\text{Li}_{0.33}\text{TiS}_2$ and $\text{Li}_{0.94}\text{TiS}_2$. *Solid State Commun* 36:345–348
 72. Hibma T (1980) X-ray study of the ordering of the alkali ions in the intercalation compounds Na_xTiS_2 and Li_xTiS_2 . *J Solid State Chem* 34:97–106
 73. Murray JL (1986) The S-Ti (sulfur-titanium) system. *Bull Alloy Phase Diagrams* 7:156–163
 74. Bale CW (1989) The Li-Ti (lithium-titanium) system. *Bull Alloy Phase Diagrams* 10:135–138
 75. Okamoto H (1995) The Li-S (lithium-sulfur) system. *Bull Alloy Phase Diagrams* 16:94–97
 76. Oshima K, Yokoyama M, Hinode H, Wakihara M, Taniguchi M (1986) Synthesis of titanium sulfides under high pressure. *J Solid State Chem* 65:392–395